ISSN: 2790-5209 DOI: 10.56028/fesr.1.2.17

Kinematic analysis of intelligent petrochemical fluid handling arm

Haonan Yan*, Lijun Meng, Wenbin Shu

School of Mechanical Engineering, Xijing College

*yhn529379556@163.com

Abstract

In view of the low degree of automation of fluid transfer device in China's petrochemical industry, this paper designs and develops an intelligent fluid transfer operator arm instead of manual operation and draws its three-dimensional model based on the common structure type of land-based fluid loading and unloading arm in the current market. The kinematic model of the arm was developed based on the Denavit-Hartenberg method, and the forward and inverse kinematics were analyzed; then the Jacobi matrix of the arm was obtained based on the chi-square transformation matrix and vector product method. Finally, the positive kinematic simulation was carried out by using the Robotics Toolbox toolkit in Matlab software, and the conclusion that the linkage coordinate system established by the D-H method is consistent with the actual structure of the manipulator arm in this paper.

Keywords

D-H method; forward and inverse kinematic analysis; Jacobi matrix.

ISSN: 2790-5209 DOI: 10.56028/fesr.1.2.17

1. Preface

Most of the refining companies have been using manual crane pipes (as the name implies, a kind of pipe that can be telescoped and moved) to transfer crude oil, asphalt, benzene and other petrochemical fluids from large central storage tankers for refilling, but from the use of the manual crane pipes have the following main problems: 1. The top of the tank is arc-shaped, rain and snow operation is very easy to cause the staff standing on the top of its fall; 3. filling pendant internal and external residual liquid often dripping in the top of the tank and the ground, resulting in environmental pollution. In order to avoid the above problems, the market has also put into use some automatic loading platform to replace the manual operation to complete the fluid transfer refilling. The problem of automatic oil scraping and oil-holding has not been solved, and it does not meet the requirements of green environment protection. With the increasing concern for industrial production efficiency, operational safety and ecological environmental protection, an intelligent fluid loading and docking device that meets the requirements of green environment protection is the "immediate need" for the petrochemical industry to link the production, transportation and marketing of petrochemical fluids.

Based on the recent use of various types of land-based fluid loading arms in petrochemical industry, this paper constructs a robot arm model with four rotary joints, and accordingly establishes the kinematic model of the studied robot arm using the D-H parameter method and performs the forward and inverse kinematic analysis; then, the Jacobi matrix of the robot arm is obtained based on the chi-square transformation matrix and vector product method obtained from the forward kinematic analysis. Finally, the Robot Toolbox module of Matlab software was used to import the robot arm model and verify the positive kinematic simulation, and the kinematic model based on the D-H method was found to be consistent with the actual structure of the arm in this paper.

2. Kinematic analysis

2.1. Kinematic modeling

The three-dimensional model of the robotic arm is shown in Fig.1,and the mathematical models between its adjacent joints based on the D-H method are shown in Fig.2 and Fig.3 accordingly. The relevant parameters of the robotic arm based on the D-H method are shown in Table 1.

ISSN: 2790-5209 DOI: 10.56028/fesr.1.2.17

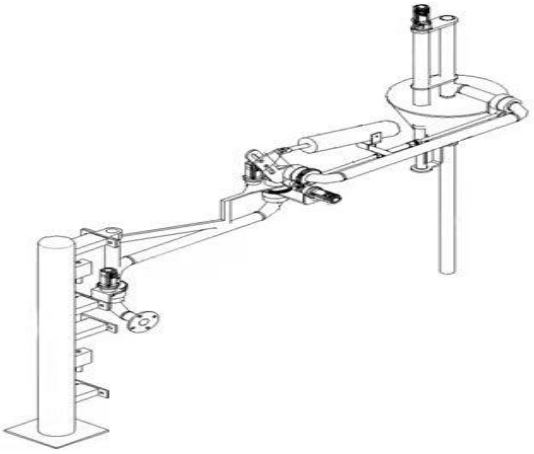

Figure1 3D model of the robot arm

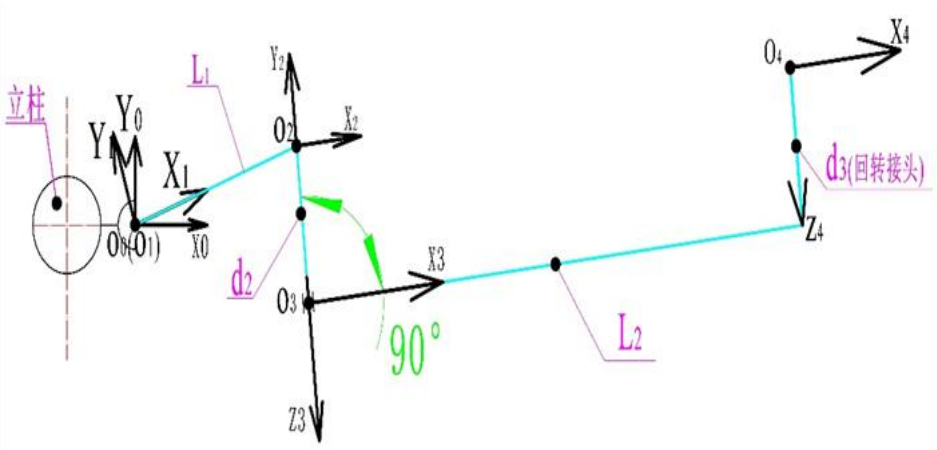

Figure2 Coordinate system of each linkage parameter in the robotic arm (I)

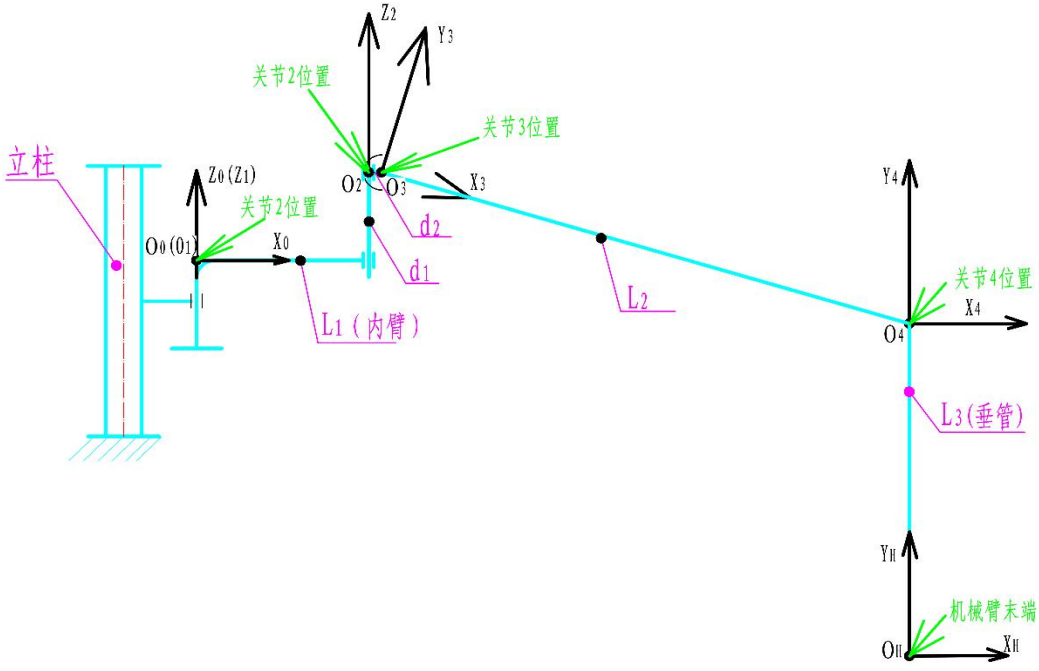

Figure3 Coordinate system of each linkage parameter in the robot arm (II)

Table 1 Table of D-H parameters of the robotic arm

ISSN: 2790-5209 DOI: 10.56028/fesr.1.2.17

Joint Serial No.	Joint Corner（θ_i）	Joint deflection d_i(mm)	Linkage length a_{i1}(mm)	Torsionangle α_{i-1}	Angular range of motion of each joint
1	θ_1（Variable）	0	0	0°	-90°~135°
2	θ_2（Variable）	d_1(650)	L_1(1000)	0°	-120°~120°
3	θ_3（Variable）	d_2(650)	0	90°	-45°~+45°
4	θ_4（Variable）	d_3(650)	L_2(3600)	0°	±15°

2.2. Positive kinematic analysis

If the rotation angle of each joint of the robot arm is known, and then the spatial position and attitude of the end of the robot arm with respect to the base coordinate are calculated, it is the positive kinematic analysis. Based on the theoretical basis related to the D-H parametric method and the flush coordinate transformation matrix and the names of each coordinate system in the robot arm model in Fig. 2 and Fig. 3, the general expression of the link transformation matrix between the two adjacent linkage links i-1 and linkage i is:

$$ {}^{i-1}_{i}\boldsymbol{T} = \begin{bmatrix} \cos(\theta_i) & -\sin(\theta_i) & 0 & a_{i-1} \\ \sin(\theta_i)\cos(\alpha_{i-1}) & \cos(\theta_i)\cos(\alpha_{i-1}) & -\sin(\alpha_{i-1}) & -d_i\sin(\alpha_{i-1}) \\ \sin(\theta_i)\sin(\alpha_{i-1}) & \cos(\theta_i)\sin(\alpha_{i-1}) & \cos(\alpha_{i-1}) & d_i\cos(\alpha_{i-1}) \\ 0 & 0 & 0 & 1 \end{bmatrix} \quad (1) $$

Based on the expression of the transformation matrix in Eq.1 above, the expression of the positive kinematic solution corresponding to Fig.1 is based on

$$ {}^{0}_{H}\boldsymbol{T} = {}^{0}_{1}\boldsymbol{T}(\theta_1)\times{}^{1}_{2}\boldsymbol{T}(\theta_2)\times{}^{2}_{3}\boldsymbol{T}(\theta_3)\times{}^{3}_{4}\boldsymbol{T}(\theta_4)\times{}^{4}_{H}\boldsymbol{T} = \begin{bmatrix} n_x & r_x & u_x & q_x \\ n_y & r_y & u_y & q_y \\ n_z & r_z & u_z & q_z \\ 0 & 0 & 0 & 1 \end{bmatrix} \quad (2) $$

where the expression for the end attitude of the robot arm：

$n_x = \cos(\theta_{34})\cos(\theta_{12})$、$n_y = \cos(\theta_{34})\sin(\theta_{12})$、$n_z = \sin\theta_{34}$；$r_x = -\sin(\theta_{12})$、$r_y = \cos(\theta_{12})$、$r_z = 0$；

$u_x = -\cos(\theta_{12})\sin(\theta_{34})$、$u_y = -\sin(\theta_{12})\sin(\theta_{34})$、$u_z = \cos\theta_{34}$；

Robotic arm end position equation：

$$ q_x = L_1\cos(\theta_1) + L_2\cos(\theta_{12})\cos(\theta_3) + L_3\cos(\theta_{12})\sin(\theta_{34}) $$

$$ q_y = L_1\sin(\theta_1) + L_2\sin(\theta_{12})\cos(\theta_3) + L_3\sin(\theta_{12})\sin(\theta_{34}) \quad (3) $$

ISSN: 2790-5209 DOI: 10.56028/fesr.1.2.17

$$q_z = d_1 + L_2 \sin(\theta_3) - L_3 \times \cos(\theta_{34})$$

In the above expression, $\theta_{12} = \theta_1 + \theta_2$、$\theta_{34} = \theta_3 + \theta_4$。

2.3. Inverse kinematic analysis

From a practical engineering point of view, it is more important to perform inverse kinematic analysis of the manipulator arm, and the inverse kinematic solution is the basis for robot motion planning and trajectory control. Compared with the forward kinematic analysis of the robot, the inverse kinematic analysis of the robot refers to the process of finding the analytical solution of each joint parameter with the knowledge of the geometric structure parameters and end contact posture of each joint contained in the robot. Considering that the joints in the robot arm are all rotary joints, the expressions for the joint angles obtained from the inverse kinematics are as follows due to the space limitation of the paper:

$$\theta_1 = \theta_{12} - \theta_2 = A\tan 2(-r_x, r_y) - A\tan 2\left(\frac{-p_x r_x - p_y u_y}{L_1}, \frac{L_3\left((\pm\sqrt{\frac{L_2^2 - (p_z - d_2)^2}{L_2^2}} + nz\right) + p_x r_y - p_y r_x\right)}{a_1}\right)$$

$$\theta_2 = A\tan 2\left(\frac{-p_x r_x - p_y r_y}{L_1}, \frac{L_3\left((\pm\sqrt{\frac{L_2^2 - (p_z - d_2)^2}{L_2^2}}) + p_x r_y - p_y r_x\right)}{L_1}\right)$$

$$\theta_3 = A\tan 2\left(\frac{p_z - d_2 - L_3 u_z}{L_2}, \pm\sqrt{\frac{L_2^2 - (p_z - d_2 - L_3 u_z)^2}{L_2^2}}\right)$$

$$\theta_4 = \theta_{34} - \theta_3 = A\tan 2(n_z, u_z) - A\tan 2\left(\frac{p_z - d_2 - L_3 u_z}{L_2}, \pm\sqrt{\frac{L_2^2 - (p_z - d_2 - L_3 u_z)^2}{L_2^2}}\right) \quad (4)$$

Observing the results of Eq.4, it can be found that the number of solutions obtained from the inverse kinematic analysis is not unique. Although the number of solutions of the inverse kinematic solution is diverse, the number of solutions that satisfy the conditions will be reduced accordingly due to the structural limitations of the arm itself, and a set of solutions should be found that meet the actual working requirements of the arm, i.e., closest to the current position of the arm, or considering the obstacle avoidance requirements.

2.4. Positive kinematic simulation

Two sets of joint vectors consisting of joint angles are randomly given, where q1 = [15°, 22.5°, 7.5°, 15°] and q2 = [30°, 22.5°, 15°, -7.5°], and the end positions of the robot arm are obtained by using the positive kinematic equation with the corresponding joint angles given in the Matlab software interface, and then the two sets of solutions obtained in turn are The two sets of solutions are then verified in turn. The two approaches based on the two sets of joint variables were used to find that the arm model built by the Matlab software matches the actual arm model built by the 3D software.

The end positions of the robotic arm for two different sets of joint angles based on the positive

ISSN: 2790-5209 DOI: 10.56028/fesr.1.2.17

kinematic analysis are shown in Eqs. 6 and 7.

$$T_1 = \begin{bmatrix} 0.7330 & -0.6088 & -0.3036 & 4738.7336 \\ 0.5624 & 0.7934 & -0.2330 & 3153.7963 \\ 0.3827 & 0 & 0.9239 & -1744.1323 \\ 0 & 0 & 0 & 1 \end{bmatrix} \quad (5)$$

$$T_2 = \begin{bmatrix} 0.6036 & -0.7934 & -0.7946 & 3229.2155 \\ 0.7866 & 0.6088 & -0.1036 & 3579.7692 \\ 0.1305 & 0 & 0.9914 & 1491.7305 \\ 0 & 0 & 0 & 1 \end{bmatrix} \quad (6)$$

Correspondingly, the expressions of the two sets of solutions obtained based on the Robot Toolbox module of the MATLAB software are shown in Fig. 4 and Fig. 5, respectively.

```
T1 =
    0.7330   -0.6088   -0.3036    4739
    0.5624    0.7934   -0.2330    3154
    0.3827         0    0.9239   -1744
         0         0         0       1
```

Figure 4 The corresponding chi-square transformation matrix of the joint vector (q1)

```
T2 =
    0.6036   -0.7934   -0.0795    3229
    0.7866    0.6088   -0.1036    3580
    0.1305         0    0.9914   -1492
         0         0         0       1
```

Fig. 5 Qi transformation matrix corresponding to joint vector (q2)

Accordingly, the end positions presented by the above two sets of robotic arms at different joint angles are shown in Fig. 4 and Fig. 5, respectively.

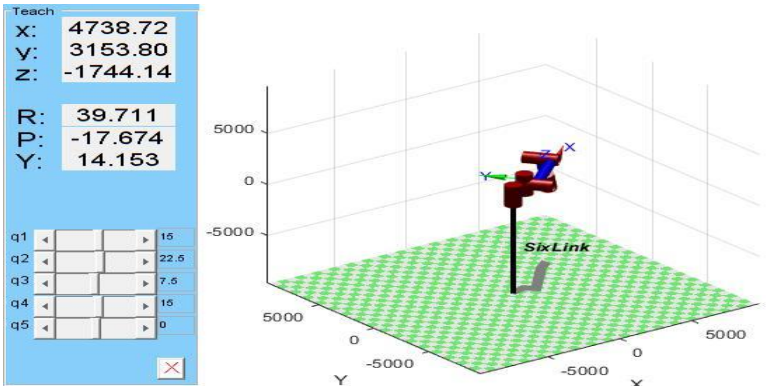

Fig. 4 Joint vector (q1) corresponding to the robotic arm presentation pose

ISSN: 2790-5209 DOI: 10.56028/fesr.1.2.17

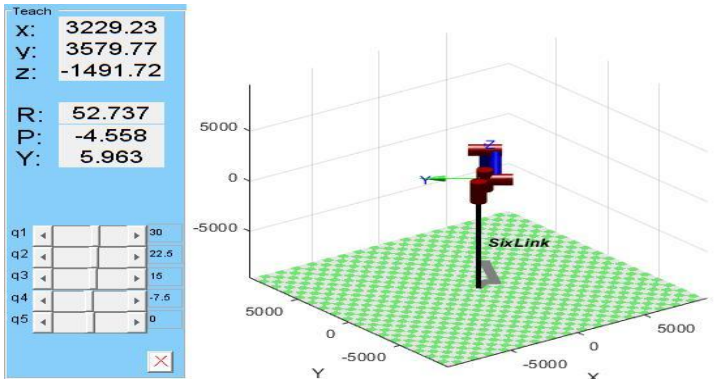

Fig. 5 The joint vector (q2) corresponding to the robotic arm presentation pose

3. Jacobi matrix solution

As a reflection of the relationship between the differential motion of individual joints in a robotic arm and the differential motion of the end of the arm, the Jacobi matrix can also be used to represent a linear mapping of the joint space velocity to the operation space velocity, for which the Jacobi matrix of the robotic arm model in this paper will be solved. There are three most common methods to solve the Jacobi matrix, i.e., vector product method, differential transformation method and spiral motion solution method based on spin theory. Considering that the end coordinate system of the robot arm is in the same attitude with the base coordinate system, the method of solving the Jacobi matrix in this paper is the vector product method. Since the joints in the robotic arm in this paper are all rotational joints, the general expressions of the columns of its Jacobi matrix are

$$\boldsymbol{J}_i = \begin{bmatrix} \boldsymbol{Z}_i \times {}^{i}\boldsymbol{p}_{\mathrm{n}}{}^{0} \\ \boldsymbol{Z}_i \end{bmatrix} = \begin{bmatrix} \boldsymbol{Z}_i \times ({}^{0}_{i}\boldsymbol{R}\,{}^{i}\boldsymbol{P}_{\mathrm{n}}) \\ \boldsymbol{Z}_i \end{bmatrix} \tag{8}$$

In Eq. 8, Zi denotes the z-axis unit vector of the coordinate system {i} with respect to the base scale system {0}, and denotes the representation of the position vector of the coordinate origin of the end of the robot arm in the base scale system {0} with respect to the coordinate system {i},i.e.

$${}^{i}\boldsymbol{p}_{\mathrm{n}}{}^{0} = {}^{0}_{i}\boldsymbol{R}\,{}^{i}\boldsymbol{P}_{\mathrm{n}} \tag{9}$$

Given the number of joints contained in the robotic arm, the end positions obtained from the positive kinematic analysis and Eqs. 7 and 8, the expression of the Jacobi matrix can be obtained as

$$\boldsymbol{J} = \begin{bmatrix} \boldsymbol{J}_1 & \boldsymbol{J}_2 & \boldsymbol{J}_3 & \boldsymbol{J}_4 \end{bmatrix} \tag{10}$$

In equation 10，

$$\boldsymbol{J}_1 = \begin{bmatrix} -sin(\theta_1+\theta_2)L_1 - sin(\theta_1+\theta_2)L_2cos(\theta_3) \\ L_1cos(\theta_1)+L_2cos(\theta_1+\theta_2)cos(\theta_3) \\ 0 \\ 0 \\ 0 \\ 1 \end{bmatrix}$$

ISSN: 2790-5209 DOI: 10.56028/fesr.1.2.17

$$\boldsymbol{J}_2=\begin{bmatrix} -L_2 sin(\theta_1+\theta_2)cos(\theta_3) \\ L_2 cos(\theta_1+\theta_2)cos(\theta_3) \\ 0 \\ 0 \\ 0 \\ 1 \end{bmatrix} \boldsymbol{J}_3=\begin{bmatrix} -L_2 cos(\theta_1+\theta_2)sin(\theta_3) \\ -L_2 sin(\theta_1+\theta_2)sin(\theta_3) \\ L_2 cos(\theta_3) \\ sin(\theta_1+\theta_2) \\ -cos(\theta_1+\theta_2) \\ 0 \end{bmatrix}, \quad \boldsymbol{J}_4=\begin{bmatrix} 0 \\ 0 \\ 0 \\ sin(\theta_1+\theta_2) \\ -cos(\theta_1+\theta_2) \\ 0 \end{bmatrix}$$

4. Conclusion

In this paper, the kinematic model of the industrial robot was first established using the D-H parametric modeling method, and then its kinematic equations were derived using the coordinate transformation matrix and solved by forward and inverse kinematics. Then, the kinematic simulation of the studied robot arm is carried out by using Matlab software robotics toolbox. Although the experimental results basically meet the expectations, the simulation verification is carried out in an ideal environment without obstacles and disturbances, while the actual working robot arm is subject to certain degree of limitations. The next tasks are: 1) how to solve the robot dynamics problem in the presence of disturbances; 2) how to plan the trajectory of the robot arm when the angular range of movement of each joint is limited; 3) how to use the robot arm to find the location of the tank opening and complete the filling operation successfully.

Reference

[1] Yushan Leng,Zilong Deng,Jun Xing. Kinematic analysis of a Matlab-based six-degree-of-freedom tandem robot[J]. Manufacturing Automation,2020,42(09):56-61.

[2] Yu Hao, Chen Gui, Ding Fei, Xu Yiyan. Research on kinematic modeling and trajectory planning of tandem robots[J]. Journal of Nanjing Engineering College (Natural Science Edition),2022,20(01):27-31.DOI:10.13960/j.issn.1672-2558.2022.01.006.

[3] Robotics;Investigators at South China University of Technology Discuss Findings in Robotics (Dynamic Modeling and Comparative Analysis of a 3-prr Parallel Robot With Multiple Lubricated Joints)[J]. Journal of Engineering,2019.

[4] Liao Liangchuang,Chen Weibin,Yan Ding,Shen Yan. Solution of inverse kinematic problem for serial robot based on screw theory[J]. ACTIVE AND PASSIVE SMART STRUCTURES AND INTEGRATED SYSTEMS XIV,2020,11376.